Supplementary Material (ESI) for Journal of Materials Chemistry

The effect of compactness on the carbothermal conversion of interpenetrating metal oxide / resorcinol-formaldehyde nanoparticle networks to porous metals and carbides

Nicholas Leventis*, NaveenChandrasekaran, Anand G. Sadekar, SudhirMulik, and CharikliaSotiriou-Leventis*

Department of Chemistry, Missouri University of Science and Technology, Rolla, MO 65409, U.S.A. (leventis@mst.edu; cslevent@mst.edu)

Electronic Supplementary Information

Figure S.1. Solids ^{13}C NMR of representative native and X-RF-MOx systems (cases shown, M: Sn, Cu, Hf)

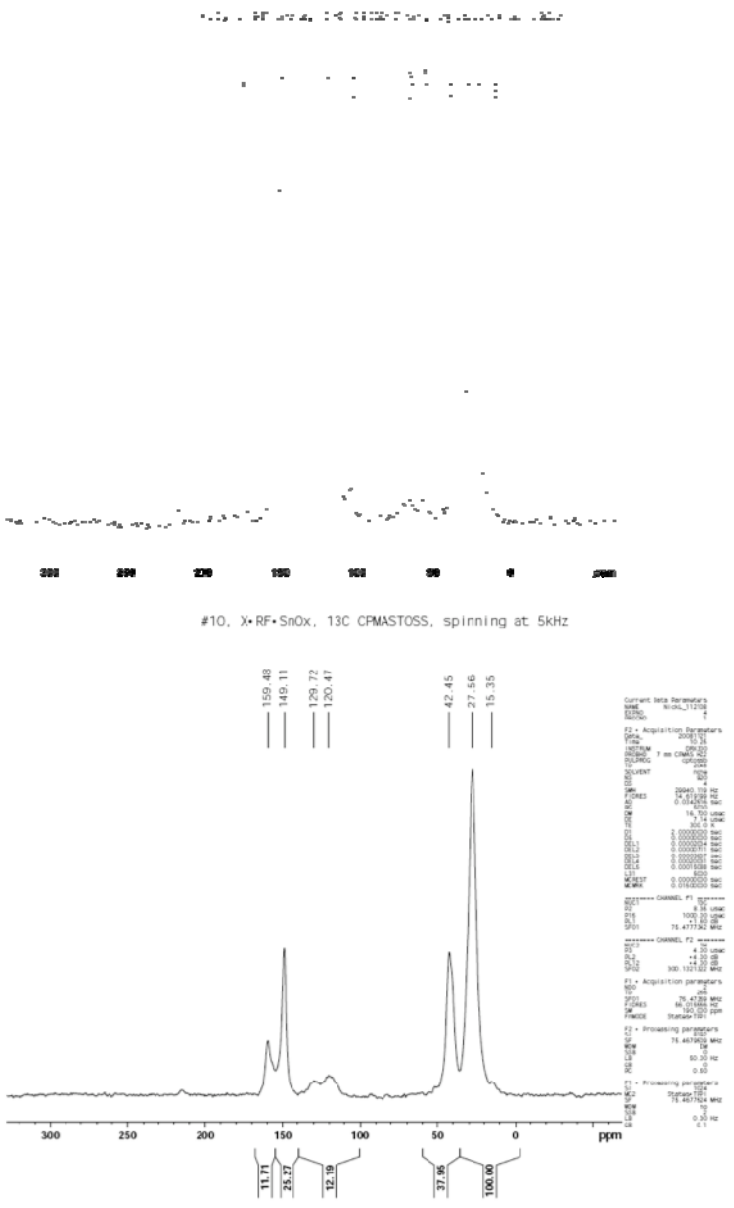

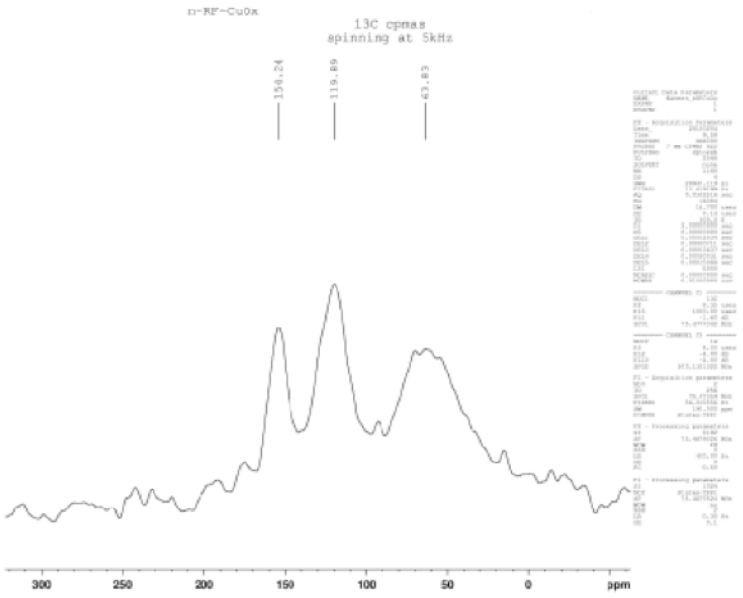
13C cpmas
spinning at 5kHz
158.24
119.89
63.83
300
250
200
150
100
50
0
ppm

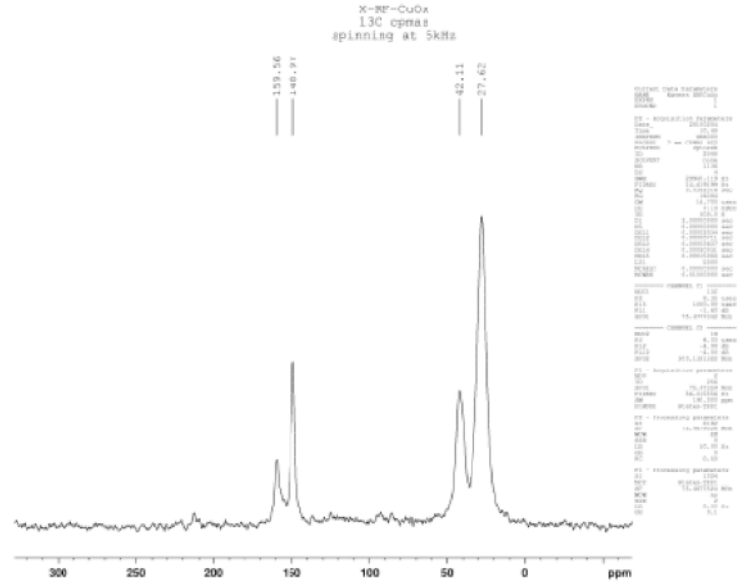
X-RF-CuOx
13C cpmas
spinning at 5kHz
159.56
148.97
40.11
27.62
300
250
200
150
100
50
0
ppm

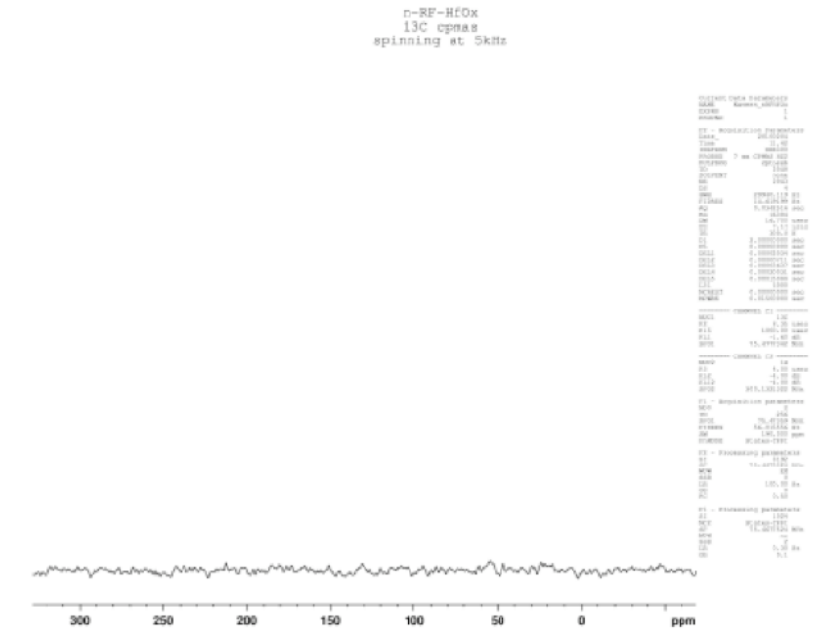
n-RF-HfOx
13C cpmas
spinning at 5kHz
300
250
200
150
100
50
0
ppm

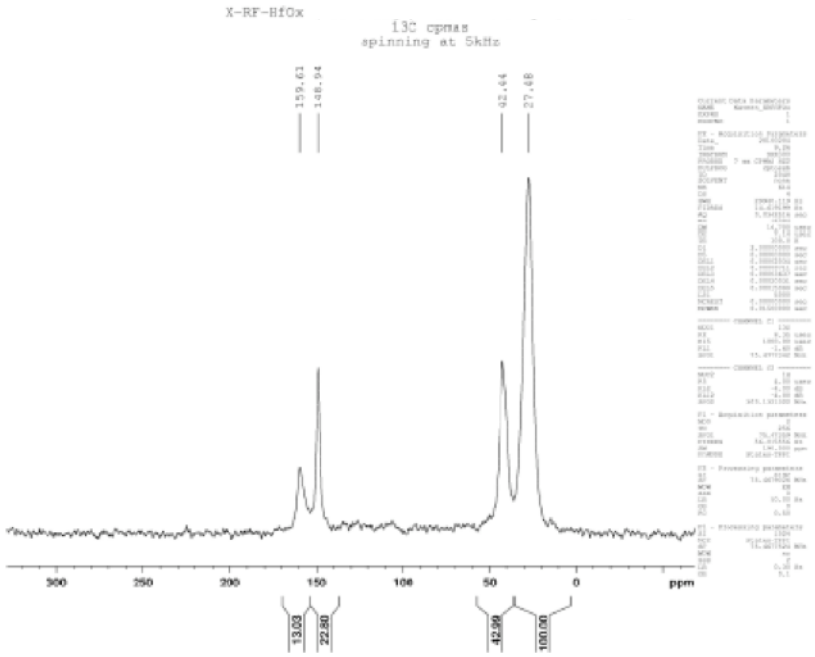
X-RF-HfOx
13C cpmas
spinning at 5kHz
159.61
148.94
92.44
27.48
300
250
200
150
100
50
0
ppm
13.03
22.80
42.99
100.00

Figure S.2. XRD and EDS data as a function of pyrolysis temperature (under Ar) for the smeltable RF-MOx systems (M: Fe, Co, Ni, Cu) in their native aerogel (top), xerogel (middle) and X-aerogel (bottom) forms

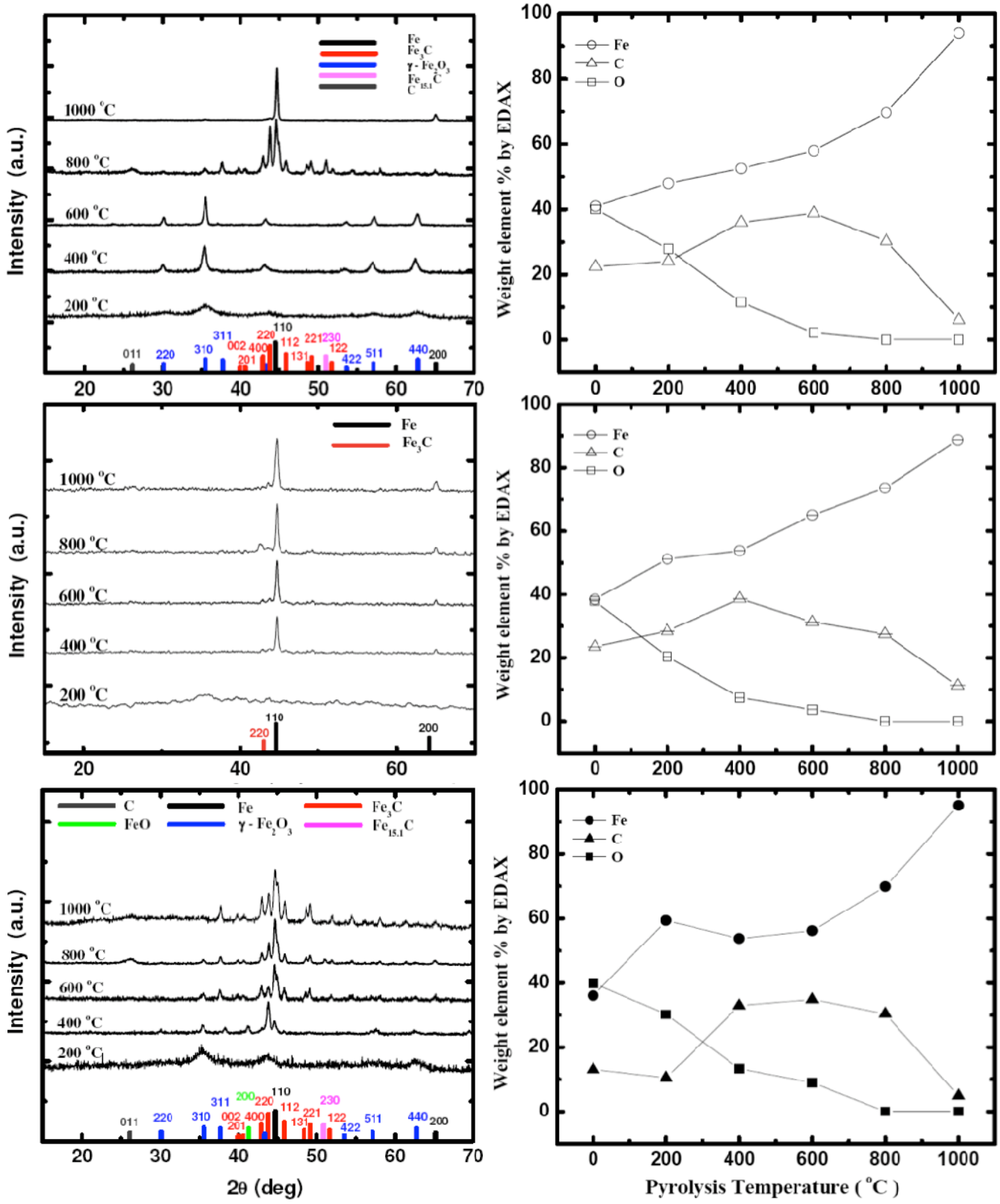

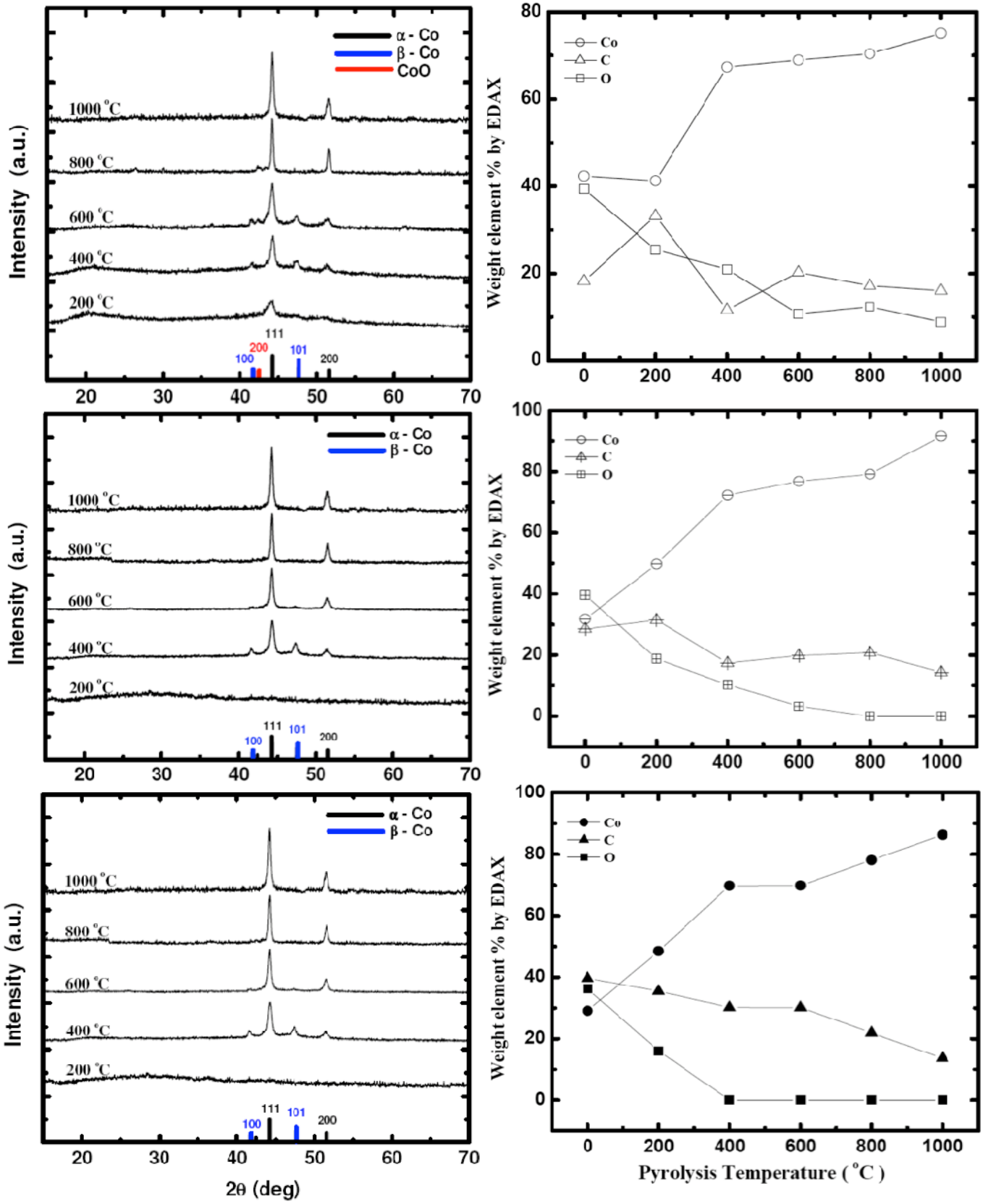
α - Co
β - Co
CoO
1000 °C
800 °C
600 °C
400 °C
200 °C
111
200
100
101
200
Intensity (a.u.)
20
30
40
50
60
70
Co
C
O
Weight element % by EDAX
0
20
40
60
80
0
200
400
600
800
1000
α - Co
β - Co
1000 °C
800 °C
600 °C
400 °C
200 °C
111
101
100
200
Intensity (a.u.)
Co
C
O
Weight element % by EDAX
0
20
40
60
80
100
0
200
400
600
800
1000
α - Co
β - Co
1000 °C
800 °C
600 °C
400 °C
200 °C
111
101
100
200
Intensity (a.u.)
2θ (deg)
Co
C
O
Weight element % by EDAX
0
20
40
60
80
100
0
200
400
600
800
1000
Pyrolysis Temperature (°C)

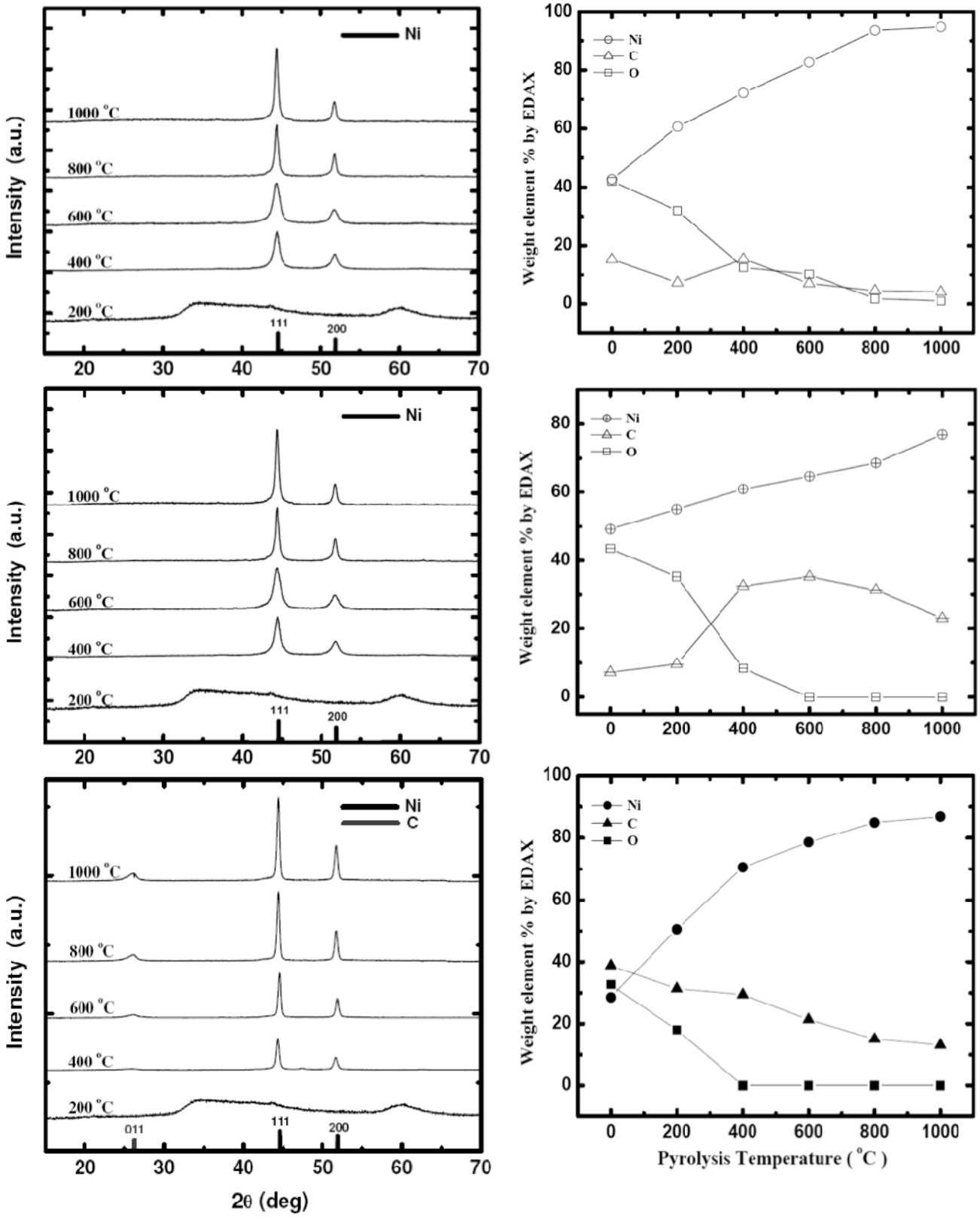
Ni
1000 °C
800 °C
600 °C
400 °C
200 °C
111
200
Intensity (a.u.)
20 30 40 50 60 70
Ni
C
011
2θ (deg)
Weight element % by EDAX
Ni
C
O
0 200 400 600 800 1000
Pyrolysis Temperature (°C)

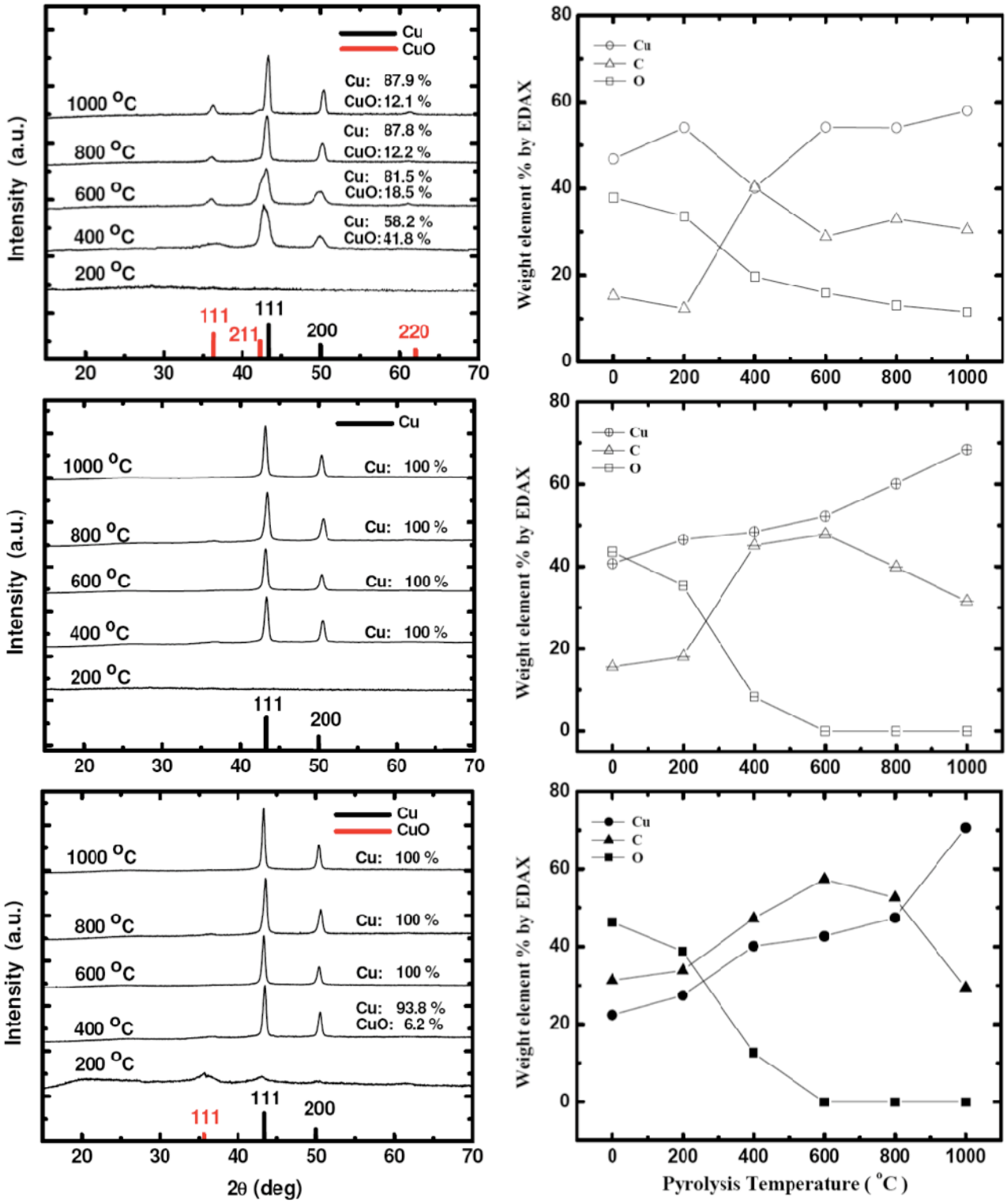
Cu
CuO
1000 °C
800 °C
600 °C
400 °C
200 °C
Cu: 87.9 %
CuO:12.1 %
Cu: 87.8 %
CuO:12.2 %
Cu: 81.5 %
CuO:18.5 %
Cu: 58.2 %
CuO:41.8 %
111
211
111
200
220
Intensity (a.u.)
Cu: 100 %
Cu: 93.8 %
CuO: 6.2 %
2θ (deg)
Weight element % by EDAX
C
O
Pyrolysis Temperature (°C)

Figure S.3. XRD data as a function of the pyrolysis temperature (under Ar) for the RF-MOx systems convertible to carbides (M: Ti, Hf); Top: native aerogels; Middle: xerogels; Bottom: X-aerogels

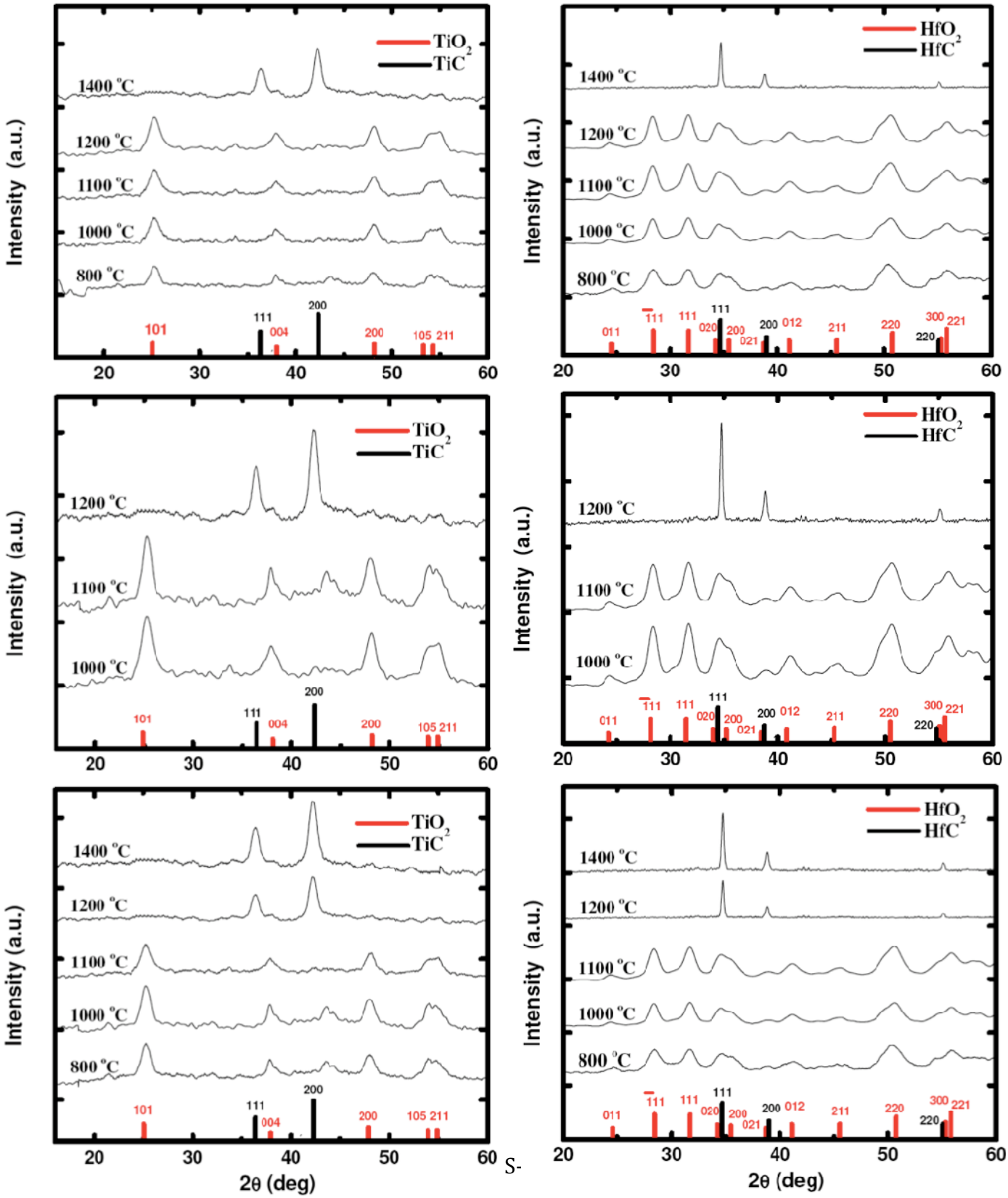

S-

Figure S.4. XRD data as a function of the pyrolysis temperature (under Ar) for RF-YOx and RF-DyOx; Top: native aerogels; Middle: xerogels; Bottom: X-aerogels

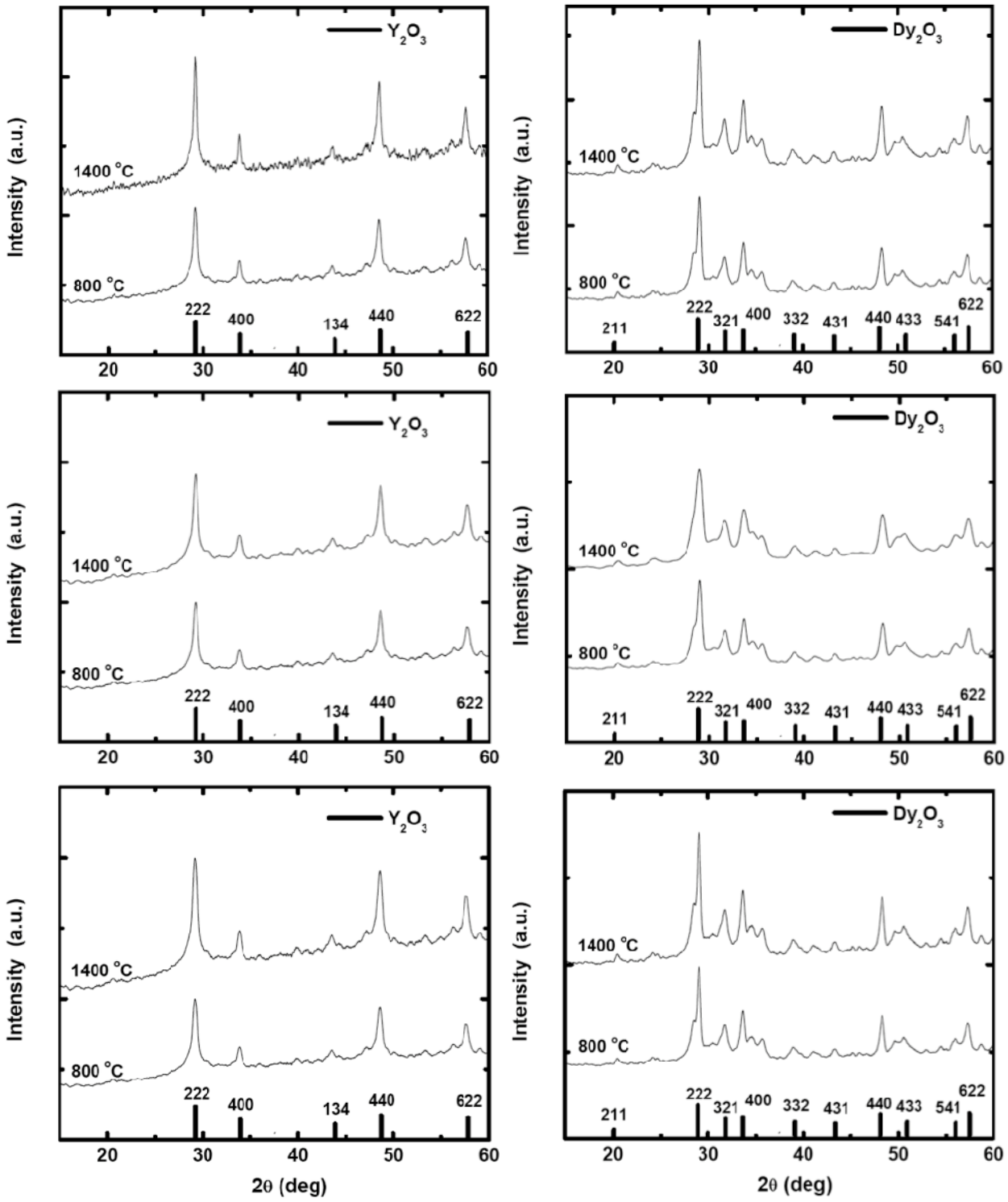

Table S.1. Property evolution upon pyrolysis of the RF-FeOx system

sample	diameter (cm) [a]	shrinkage (%) [a,b]	bulk density, ρ_b (g cm^{-3}) [a]	skeletal density, ρ_s (g cm^{-3}) [c]	porosity, Π(% void space)	BET surface area, σ (m^2 g^{-1})	average pore diameter (nm) [d]	particle radius, r (nm) [e]
n-RF-FeOx								
RT	0.946±0.01	13.2±1.31	0.047±0.001	2.86±0.12	98	298	33.8 [26.2]	3.5
800°C	0.52±0.01	48.2±0.28	0.15±0.05	3.74±0.23	95.9	141	54.9 [55.5]	5.6
1000°C		5.40±0.27		130	57.6 [63.7]	4.3		
Xero-RF-FeOx								
RT	0.38±0.02	63.4±0.49	1.00±0.04	1.81±0.01	45	184	4.8 [3.2]	9.0
800°C	0.32±0.01	73.2±0.12	1.28±0.01	3.54±0.30	64.1	51	5.2 [7.4]	16.6
1000°C	0.22±0.01	78.8±0.32	1.73±0.18	4.89±0.28	66.3	82.5	5.8 [6.4]	7.4
X-RF-FeOx								
RT	1.00±0.03	6.16±0.58	0.42±0.01	1.42±0.01	71	80	28.8 [33.1]	26.4
800°C	0.49±0.01	52.8 ±0.22	0.16±0.02	4.15±0.44	96.1	174	40.8 [42.9]	4.2
1000°C	0.48±0.02	54.0±0.28	0.192±0.003	4.40±0.40	95.4	157	45.7 [65.9]	4.3

[a]. Average of 3 samples. (Mold diameter: 1.04 cm.) [b]. Shrinkage = 100 × (mold diameter– sample diameter)/(mold diameter). [c]. Single sample, average of 50 measurements. [d]. By the BJH-desorption method; in brackets: width at half maximum in nm [e]. Calculated via $r = 3/\rho_s\sigma$.

Table S.2. Property evolution upon pyrolysis of the RF-CoOx system

sample	diameter (cm) [a]	shrinkage (%) [a,b]	bulk density, ρ_b (g cm^{-3}) [a]	skeletal density, ρ_s (g cm^{-3}) [c]	porosity, Π(% void space)	BET surface area, σ (m^2 g^{-1})	average pore diameter (nm) [d]	particle radius, r (nm) [e]
n-RF-CoOx								
RT	0.783±0.024	21.6±2.51	0.082±0.001	2.34±0.19	97	143	36.3 [45.3]	9.0
800°C	0.64±0.03	38.4±0.03	0.188±0.001	3.71±0.81	95.85	554.7	28.2 [31.8]	1.5
1000°C	0.56±0.02	46.1±0.04	0.28±0.08	3.80±0.46	94.3	276.1	23.4 [29.8]	2.9
Xero-RF-CoOx								
RT	0.43±0.04	58.6±0.53	0.81±0.12	1.93±0.04	35 123	4.8 [3.5]	12.6	
800°C	0.40±0.01	61.5±0.23	1.53±0.08	3.83±0.90	59.8	46.8	5.4 [4.8]	16.7
1000°C	0.34±0.03	67.3±0.17	1.89±0.22	3.98±0.24	52.8	41.2	5.1 [6.4]	18.3
X-RF-CoOx								
RT	0.91±0.02	6.16±0.58	0.37±0.03	1.42±0.05	71	52	22.3 [26.2]	40.9
800°C	0.61±0.01	41.3 ±0.22	0.327±0.002	3.14±0.17	89.5	108	5.6 [5.4]	8.8
1000°C	0.64±0.02	38.4±0.28	0.48±0.01	4.78±0.01	89.9	31	7.1 [6.7]	20.2

[a]. Average of 3 samples. (Mold diameter: 1.04 cm.). [b]. Shrinkage = 100 × (mold diameter– sample diameter)/(mold diameter). [c]. Single sample, average of 50 measurements. [d]. By the BJH-desorption method; in brackets: width at half maximum in nm [e]. Calculated via $r = 3/\rho_s\sigma$.

Table S.3. Property evolution upon pyrolysis of the RF-NiOx system

sample	diameter (cm) [a]	shrinkage (%) [a,b]	bulk density, ρ_b (g cm^{-3}) [a]	skeletal density, ρ_s (g cm^{-3}) [c]	porosity, Π(% void space)	BET surface area, σ (m^2 g^{-1})	average pore diameter (nm) [d]	particle radius, r (nm) [e]
n-RF-NiOx								
RT	0.69±0.015	29.7±1.25	0.059±0.003	2.59±0.13	98	309	22.9 [24.3]	3.7
800°C	0.57±0.02	45.1±0.02	0.168±0.005	4.04±0.92	96.0	303	17.9 [21.4]	2.5
1000°C	0.46±0.02	55.7±0.03	0.22±0.03	3.94±0.57	95.7	426	15.6 [18.4]	1.8
Xero-RF-NiOx								
RT	0.55±0.02	47.1±0.32	1.24±0.07	1.87±0.004	34	-----		
800°C	0.51±0.01	50.9±0.29	0.35±0.03	2.27±0.06	84.8	42.7	5.3 [6.8]	31.0
1000°C	0.48±0.01	53.8±0.18	0.58±0.23	2.83±0.07	79.4	22.3	5.7 [6.3]	47.5
X-RF-NiOx								
RT	0.93±0.04	8.6±1.1	0.397±0.015	1.38±0.005	69	150	17.7 [15.0]	14.5
800°C	0.52±0.03	50 ±1.18	0.405±0.017	2.19±0.12	81.6	177	14.6 [17.2]	7.7
1000°C	0.54±0.02	48.07±0.37	0.32±0.02	2.71±0.03	88.0	116	6.5 [7.1]	9.5

[a]. Average of 3 samples. (Mold diameter: 1.04 cm.) [b]. Shrinkage = 100 × (mold diameter– sample diameter)/(mold diameter). [c]. Single sample, average of 50 measurements. [d]. By the BJH-desorption method; in brackets: width at half maximum in nm [e]. Calculated via $r = 3/\rho_s\sigma$.

Table S.4. Property evolution upon pyrolysis of the RF-SnOx system

sample	diameter (cm) [a]	shrinkage (%) [a,b]	bulk density, ρ_b (g cm^{-3}) [a]	skeletal density, ρ_s (g cm^{-3}) [c]	porosity, Π(% void space)	BET surface area, σ (m^2 g^{-1})	average pore diameter (nm) [d]	particle radius, r (nm) [e]
n-RF-SnOx								
RT	0.756±0.005	24.3±0.57	0.135±0.031	2.58±0.13	95	147	37.1 [41.4]	7.9
800°C	0.59±0.01	43.2±0.33	0.158±0.08	3.85±0.25	95.8	722	22.8 [31.4]	1.1
1000°C	0.62±0.07	44.4±0.23	0.185±0.01	3.70±0.06	96.1	548	26.3 [38.2]	1.5
Xero-RF-SnOx								
RT	0.37±0.03	64.4±0.58	1.15±0.08	1.85±0.02	39	-----	-----	-----
800°C	0.32±0.01	69.2±0.16	1.73±0.04	1.96±0.08	10.5	176	3.4 [4.7]	8.7
1000°C	0.30±0.06	71.1±0.44	1.41±0.18	2.64±0.20	46.6	147	5.9 [7.8]	7.7
X-RF-SnOx								
RT	0.86±0.01	13.8±0.42	0.31±0.01	1.27±0.004	77	60	31.6 [34.7]	39.3
800°C	0.63±0.01	39.4 ±0.12	0.48±0.04	2.90±0.12	84.5	6.61	38.2 [42.4]	4.51
1000°C	0.64±0.02	38.4±0.18	0.595±0.002	3.78±0.08	87.0	------	-----	-----

[a]. Average of 3 samples. (Mold diameter: 1.04 cm.) [b]. Shrinkage = 100 × (mold diameter– sample diameter)/(mold diameter). [c]. Single sample, average of 50 measurements. [d]. By the BJH-desorption method; in brackets: width at half maximum in nm [e]. Calculated via $r = 3/\rho_s\sigma$.

Table S.5. Property evolution upon pyrolysis of the RF-CuOx system

sample	diameter (cm) [a]	shrinkage (%) [a,b]	bulk density, ρ_b (g cm^{-3}) [a]	skeletal density, ρ_s (g cm^{-3}) [c]	porosity, Π(% void space)	BET surface area, σ (m^2 g^{-1})	average pore diameter (nm) [d]	particle radius, r (nm) [e]
n-RF-CuOx								
RT	0.903±0.021	16.3±1.92	0.083±0.009	2.65±0.14	98	189	43.6 [49.6]	6.0
800°C	0.66±0.03	36.5±0.15	0.112±0.08	3.6±0.35	96.8	183	33.7 [40.7]	4.6
1000°C	0.64±0.02	38.4±0.21	0.191±0.006	4.80±0.8	96.0	175	47.8 [33.6]	3.6
Xero-RF-CuOx								
RT	0.496±0.055	52.3±1.2	1.33±0.009	2.01±0.29	34	159	4.7 [3.2]	9.4
800°C	0.29±0.03	72.1±0.14	1.13±0.01	3.81±0.13	70.3	62	5.3 [5.8]	12.7
1000°C	0.31±0.02	70.2±0.27	1.42±0.22	3.93±0.17	63.8	55	4.7 [5.3]	13.8
X-RF-CuOx								
RT	0.97±0.02	10.5±1.96	0.42±0.05	1.37±0.003	71	21	38.9 [45.2]	30.8
800°C	0.41±0.04	60.5±0.18	0.694±0.002	2.40±0.09	80.5	54	48.9 [51.6]	23.1
1000°C	0.39±0.02	62.5±0.24	0.75±0.013	2.52±0.07	86.4	79	47.8 [49.7]	15.1

[a]. Average of 3 samples. (Mold diameter: 1.04 cm.) [b]. Shrinkage = 100 × (mold diameter– sample diameter)/(mold diameter). [c]. Single sample, average of 50 measurements. [d]. By the BJH-desorption method; in brackets: width at half maximum in nm [e]. Calculated via $r = 3/\rho_s\sigma$.

Table S.6. Property evolution upon pyrolysis of the RF-CrOx system

sample	diameter (cm) [a]	shrinkage (%) [a,b]	bulk density, ρ_b (g cm^{-3}) [a]	skeletal density, ρ_s (g cm^{-3}) [c]	porosity, Π(% void space)	BET surface area, σ (m^2 g^{-1})	average pore diameter (nm) [d]	particle radius, r (nm) [e]
n-RF-CrOx								
RT	0.89±0.02	11.3±1.52	0.108±0.005	2.42±0.01	96	472	23.9 [17.1]	2.6
800°C	0.50±0.01	52.0±1.15	0.225±0.013	3.08±0.05	93	618	17.9 [22.1]	1.6
1400°C	0.48±0.04	53.8±0.32	0.284±0.008	2.51±0.04	89	252	10.8 [9.2]	4.7
Xero-RF-CrOx								
RT	0.51±0.01	50.9±1.05	1.16±0.072	1.78±0.04	35	117	4.8 [1.9]	14.4
X-RF-CrOx								
RT	0.94±0.02	6.6±1.4	0.42±0.04	1.29±0.04	68	71	29.5 [17.9]	32.2
800°C	0.43±0.02	57.0±0.15	0.39±0.01	2.78±0.05	86	368	3.81 [2.8]	2.9
1400°C	0.29±0.02	72.1±0.03	0.53±0.02	3.35±0.32	85	55	6.52 [5.8]	16.2

[a]. Average of 3 samples. (Mold diameter: 1.04 cm.) [b]. Shrinkage = 100 × (mold diameter– sample diameter)/(mold diameter). [c]. Single sample, average of 50 measurements. [d]. By the BJH-desorption method; in brackets: width at half maximum in nm [e]. Calculated via $r = 3/\rho_s\sigma$.

Table S.7. Property evolution upon pyrolysis of the RF-TiOx system

sample	diameter (cm) [a]	shrinkage (%) [a,b]	bulk density, ρ_b (g cm^{-3}) [a]	skeletal density, ρ_s (g cm^{-3}) [c]	porosity, Π(% void space)	BET surface area, σ (m^2 g^{-1})	average pore diameter (nm) [d]	particle radius, r (nm) [e]
n-RF-TiOx								
RT	0.86±0.01	12.6±0.57	0.091±0.001	2.64±0.11	96	230	23.9 [30.8]	4.9
800°C	0.37±0.01	64.4±1.28	0.366±0.012	3.56±0.01	89.7	212	13.1 [17.6]	3.9
1400°C	0.34±0.04	67.3±0.35	0.413±0.135	3.62±0.44	88.5	89	13.7 [18.7]	9.3
Xero-RF-TiOx								
RT	0.43±0.017	58.8±0.48	0.934±0.035	2.04±0.21	54	145	7.2 [4.8]	10.1
X-RF-TiOx								
RT	0.91±0.01	9.0±1.2	0.414±0.009	1.34±0.82	69	69	30.1 [15.1]	32.4
800°C	0.47±0.02	55.0±0.32	0.463±0.026	2.39±0.09	81.0	449	12.9 [13.8]	2.8
1400°C	0.31±0.12	70.2±0.12	0.59±0.01	4.85±0.15	87.7	55	5.7 [6.9]	11.2

[a]. Average of 3 samples. (Mold diameter: 1.04 cm.) [b]. Shrinkage = 100 × (mold diameter– sample diameter)/(mold diameter). [c]. Single sample, average of 50 measurements. [d]. By the BJH-desorption method; in brackets: width at half maximum in nm [e]. Calculated via $r = 3/\rho_s\sigma$.

Table S.8. Property evolution upon pyrolysis of the RF-HfOx system

sample	diameter (cm) [a]	shrinkage (%) [a,b]	bulk density, ρ_b (g cm^{-3}) [a]	skeletal density, ρ_s (g cm^{-3}) [c]	porosity, Π(% void space)	BET surface area, σ (m^2 g^{-1})	average pore diameter (nm) [d]	particle radius, r (nm) [e]
n-RF-HfOx								
RT	0.853±0.015	14.7±1.52	0.128±0.004	2.59±0.01	95	282	22.9 [37.9]	4.1
800°C	0.505±0.029	51.4±0.28	0.312±0.024	2.97±0.02	89.5	127	38.9[29.8]	8.0
1400°C	0.46±0.01	55.7±0.14	0.346±0.01	3.83±0.19	91.0	157	39.8 [20.9]	5.0
Xero-RF-HfOx								
RT	0.45±0.026	57.3±0.25	1.08±0.057	1.92±0.18	44	159	3.1 [1.0]9.8	
X-RF-HfOx								
RT	0.926±0.025	7.3±1.5	0.442±0.006	1.42±0.08	69	57	34.6 [32.7]37.1	
800°C	0.415±0.007	60.0±0.12	0.367±0.013	3.19±0.02	89.0	358	22.4[26.8]	2.62
1400°C	0.32±0.04	69.2±0.32	0.574±0.18	4.26±0.13	87.0	1.63 12.1 ----------	432	

[a]. Average of 3 samples. (Mold diameter: 1.04 cm.) [b]. Shrinkage = 100 × (mold diameter– sample diameter)/(mold diameter). [c]. Single sample, average of 50 measurements. [d]. By the BJH-desorption method; in brackets: width at half maximum in nm [e]. Calculated via $r = 3/\rho_s\sigma$.

Table S.9. Property evolution upon pyrolysis of the RF-YOx system

sample	diameter (cm) [a]	shrinkage (%) [a,b]	bulk density, ρ_b (g cm^{-3}) [a]	skeletal density, ρ_s (g cm^{-3}) [c]	porosity, Π(% void space)	BET surface area, σ (m^2 g^{-1})	average pore diameter (nm) [d]	particle radius, r (nm) [e]
n-RF-YOx								
RT	0.88±0.01	12.6±0.47	0.124±0.005	2.07±0.05	94	302	36.3 [32.1]	4.8
800°C	0.38±0.03	65.3±0.58	0.307±0.014	2.98±0.02	89.6	279	6.4 [4.8]	3.6
1400°C	0.32±0.02	69.2±0.34	0.412±0.18	2.70±0.12	84.7	88	7.8 [5.3]	12.6
Xero-RF-YOx								
RT	0.38±0.019	63.2±0.78	1.12±0.11	1.98±0.11	43122	6.0 [1.8]	12.4	
X-RF-YOx								
RT	0.94±0.05	6.0±0.18	0.330±0.003	1.25±0.01	74	99	22.3 [24.1]	24.2
800°C	0.27±0.03	74.0±0.22	0.49±0.005	4.19±0.09	88.2	555	22.1[19.8]	1.30
1400°C	0.205±0.18	80.2±0.46	0.68±0.12	5.58±0.54	87.8	----	---- [---]	------

[a]. Average of 3 samples. (Mold diameter: 1.04 cm.) [b]. Shrinkage = 100 × (mold diameter– sample diameter)/(mold diameter). [c]. Single sample, average of 50 measurements. [d]. By the BJH-desorption method; in brackets: width at half maximum in nm [e]. Calculated via $r = 3/\rho_s\sigma$.

Table S.10. Property evolution upon pyrolysis of the RF-DyOx system

sample	diameter (cm) [a]	shrinkage (%) [a,b]	bulk density, ρ_b (g cm^{-3}) [a]	skeletal density, ρ_s (g cm^{-3}) [c]	porosity, Π(% void space)	BET surface area, σ (m^2 g^{-1})	average pore diameter (nm) [d]	particle radius, r (nm) [e]
n-RF-DyOx								
RT	0.86±0.05	17.0±1.73	0.089±0.008	2.55±0.01	97	290	52.4 [32.8]	4.1
800°C	0.44±0.03	58.0±0.14	0.267±0.026	2.15±0.06	87.8	310	27.8 [31.6]	4.8
1400°C	0.39±0.01	62.5±0.32	0.384±0.04	3.31±0.60	88.4	483	6.9 [7.4]	1.9
Xero-RF-DyOx								
RT	0.51±0.025	50.6±0.82	1.17±0.031	2.18±0.24	46.3	98	7.6 [5.3]14.0	
X-RF-DyOx								
RT	0.93±0.01	6.80±1.7	0.34±0.03	1.49±0.01	68	132	45.7 [37.2] 15.2	
800°C	0.38±0.04	63.0±1.2	0.42±0.01	3.58±0.13	88.0	0.01	(---) [-----]	---
1400°C	0.27±0.03	74.0±0.2	0.67±0.01	5.00±0.14	86.5	1.91(---) [-----]	---	

a. Average of 3 samples. (Mold diameter: 1.04 cm.) b. Shrinkage = 100 × (mold diameter– sample diameter)/(mold diameter). c. Single sample, average of 50 measurements. d. By the BJH-desorption method; in brackets: width at half maximum in nm e. Calculated via $r = 3/\rho_s\sigma$.

Table S.11. Quantitative phase analysis (% w/w by XRD) of smeltable metal oxide-carbon black mixtures (1:6 mol/mol) as a function of heating temperature under Ar (in parentheses: crystallite size, nm)

	Room Temp.	400 ºC	600 ºC	800 ºC	1000 ºC
Fe_2O_3 : C (1:6 mol/mol)					
Simple mixing					
Fe_2O_3	100 (16.8)	---	---	100 (23)	100 (26.1)
Mortar and pestle					
Fe_2O_3	100 (16.8)	---	---	100 (22.8)	100 (24.5)
Ball milling					
Fe_2O_3	100 (16.3)	---	---	100 (22.6)	100 (24.7)
CoO : C (1:6 mol/mol)					
Simple mixing					
Co_2O_3	100 (18.2)	---	---	100 (19.8)	100 (22.1)
Mortar and pestle					
Co_2O_3	100 (17.7)	---	---	100 (19.5)	15 (21.8)
α-Co					85 (23.7)
Ball milling					
Co_2O_3	100 (17.8)	---	---	100 (24.2)	11.2 (26.5)
α-Co					88.8(22.9)
NiO : C (1:6 mol/mol)					
Simple mixing					
NiO	100 (17.85)	---	---	100 (18.9)	100 (22.4)
Mortar and pestle					
NiO	100 (17.8)	---	---	100 (19.1)	100 (22.6)
Ball milling					
NiO	100 (17.8)	---	---	100 (18.5)	72.5 (23.2)
Ni					27.5 (21.4)
SnO_2 : C(1:6 mol/mol)					
Simple mixing					
SnO_2	100 (18.9)	---	---	100 (20.2)	100 (23.4)
Mortar and pestle					
SnO_2	100 (18.4)	---	---	100 (20.4)	100 (22.8)
Ball milling					
SnO_2	100 (18.2)	---	---	100 (19.8)	84.5 (23.1)
Sn					15.5 (19.7)
CuO : C (1:6 mol/mol)					
Simple mixing					
CuO	100 (26.2)	100 (28.5)	100 (28.4)	89.5 (30.4)	92.5 (32.6)
Cu				11.5 (19.7)	7.5 (21.3)
Mortar and pestle					
CuO	100 (23.8)	100 (27.2)	100 (29.1)	77.0 (29.7)	66.0 (32.1)
Cu				23.0 (18.7)	34.0 (19.5)
Ball milling					
CuO	100 (22.9)	100 (25.5)	100 (26.4)	68.0 (27.8)	63.2 (28.1)
Cu		32.0 (16.4)	36.8 (18.4)		

Table S.12. Quantitative phase analysis (% w/w by XRD) of carbide-convertible metal oxide / carbon black mixtures (1:6 mol/mol) as a function of heating temperature under Ar (in parenthesis: crystallite size, nm)

	Room Temp.	1000 ºC	1100 ºC	1200 ºC	1400 ºC
Cr_2O_3 : C (1:6 mol/mol)					
Simple mixtures (not tested)					
Mortar and pestle					
Cr_2O_3	100 (26.8)	---	---	100 (29.1)	100 (35.8)
Ball milling					
Cr_2O_3	100 (25.4)			100 (27.9)	100 (34.2)
TiO_2 : C (1:6 mol/mol)					
Simple mixtures (not tested)					
Mortar and pestle					
TiO_2	100 (21.8)	---	---	100 (26.6)	100 (28.4)
Ball milling					
TiO_2	100 (21.6)			100 (27.2)	100 (27.9)
TiC					
HfO_2 : C (1:6 mol/mol)					
Simple mixtures (not tested)					
Mortar and pestle					
HfO_2	100 (23.8)	---	---	100 (28.3)	100 (31.2)
Ball milling					
HfO_2	100 (24.8)			100 (29.1)	100 (35.8)